Pergamon

Corrosion Science, Vol. 38, No. 9, pp. 1613–1635, 1996

0010–938X/96 $15.00 + 0.00

PII: S0010–938X(96)00076–5

A SIMPLIFIED METHOD FOR ESTIMATING CORROSION CAVITY GROWTH RATES

G. ENGELHARDT, M. URQUIDI-MACDONALD and D.D. MACDONALD

Center for Advanced Materials, The Pennsylvania State University, University Park, PA 16802, U.S.A.

Abstract—A simplified method is proposed for calculating corrosion cavity propagation rates. This method is based on an assumption that if the rate of an electrode reaction depends (in an explicit form) only on the potential, the pit growth rate depends only on the concentration of those species that determine the potential distribution near the metal within the cavity. The advantage of this method is that it permits one to predict the rates of cavity propagation without knowing various parameters, such as the equilibrium constants of some chemical reactions and diffusion coefficients of species that are present at relatively low concentrations near the electrode surface. The analytical expressions for calculating propagation rates of cylindrical and hemispherical pits are compared with available experimental data. The influence of aggressive anions on the pit propagation rate has been investigated. It is shown that transport processes in the internal environment do, in the general case, influence the kinetics of metal corrosion. Copyright © 1996 Elsevier Science Ltd

Keywords: C. crevice corrosion, C. pitting corrosion.

INTRODUCTION

One of the major theoretical problems in predicting damage due to localized corrosion is calculating the dimensions of the cavity at any given time as a function of the parameters controlling the corrosion process, such as the potential of the metal, concentration of reactant and product species, fluid velocity, temperature, etc. A general overview of the state of theoretical modeling of localized corrosion can be found in Refs[1,2]. Because of the mathematical complexity of the problem, analyses of the transfer processes occurring within corrosion cavities have generally employed the one-dimensional approximation. For example, it is often assumed, in the case of corrosion pits, that the cavity has a cylindrical shape with a depth L, which is much larger than the radius, a (Fig. 1(a) and (b)). Likewise, cracks are often viewed as being one-dimensional slots of length L, such that L is much greater than the opening displacement, w (see, for example, Refs[3–13]). Very often, only metal dissolution at the bottom is assumed (Fig. 1(a)). However, two-dimensional analyses of corroding hemispherical pits (Fig. 1(c)) have been described in Refs[14,15] for the case of a well-mixed electrolyte, and in Refs[16,17] for the case of a quiescent system, in which concentration gradients exist. In many cases, the results, which were obtained by mathematical simulation or by experimental studies of "ideal" cells, have been used to describe corrosion processes under real conditions.

Even for these cases of simplified geometry, the quantitative prediction of the propagation rate is not a simple task. For example, it has been suggested that, in the

*Center for Advanced Materials, The Pennsylvania State University, University Park, PA 16802, U.S.A.
Manuscript received 3 April 1996.

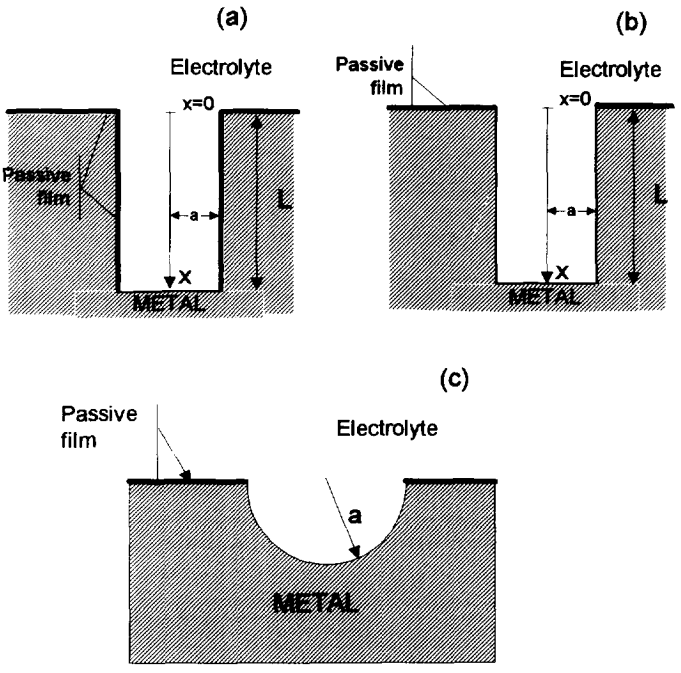

Fig. 1. A schematic diagram of the pit geometries discussed: (a) deep pit with passive walls, (b) deep pit with active walls, and hemispherical (c).

mathematical simulation of the corrosion of steels in neutral solutions, at least six species in the solution must be taken into the account.[10] These species are iron ions from the dissolution process, sodium and chloride ions (for example) that are commonly included to control the bulk conductivity, hydrogen and hydroxyl ions from the dissociation of water, and a metal hydrolysis product (e.g. $Fe(OH)^+$). The presence of terms for various chemical reactions in the balance equations for the species is a complicating factor, but frequently these terms may be eliminated by addition or subtraction of the corresponding equations. A special algorithm was used in Refs[12,13] to solve the equations directly in mass conservation form. Furthermore, for many systems, the values for the various equilibrium and kinetic parameters (for example, equilibrium constants) are not available, especially at high temperatures. Finally, for freely corroding systems, various transport and cathodic processes that occur in the external environment must be taken into account[18,19] in order to conserve charge.

For the majority of electrochemical experiments, the dependence of the characteristic pit size (for example, pit depth, L, or pit radius, a) on time, t, can be expressed by a simple equation of the following form[2,20,21]

$$L = kt^m \tag{1}$$

where k and m are empirical constants. Published values of m are very often approximately equal 1/3, 1/2, 2/3 or 1, but they can also vary over wider ranges.[20–22] As it noted in Ref.[20], the case of Ref.$m = 1/3$ is explained by ohmic polarization control outside the pit; the case of $m = 1/2$ by control due to ohmic potential drop inside the pit, when the resistance of the electrolyte is constant throughout the pit; the case of $m = 1$ is explained by the ohmic

potential drop in a salt film at the metal surface; and the case of $m = 2/3$ has not previously received a simple explanation.

Although theoretical studies, as a rule, do not present data in the form of equation (1), it would seem to be remarkable if the various models that have been proposed could rationalize the simplicity of the empirical cavity propagation laws that are observed in many cases, in spite of the complexity of the mathematical modeling process. As noted,[2] the mechanistically based models are complex to set up and, at the present stage of development, are not user-friendly. However, we have found that some models, after a little simplification that does not significantly reduce the accuracy of calculations, can yield crevice rates of the form of equation (1), and may even yield analytical expressions for parameters k and m. The principal concept in this simplification is that if the rate of the electrode reaction depends explicitly only on the local potential, the pit growth rate depends only on the concentration of those species that determine the value of electric potential near the metal surface within the cavity.

This article is devoted to examining the conditions under which it is possible to represent the cavity growth law in the form of equation (1). The case of a deep, one-dimensional pit with passive walls (Fig. 1(a)) will be investigated first. We will then use the results to describe corrosion processes in deep cavities with active walls and in hemispherical pits. We emphasize that our initial analysis applies to the cavities that are held under potentiostatic control, where the potential at the cavity mouth is the control potential, and not to the more general case of a freely corroding system, such as that treated in Refs[18,19]. However, later in this paper we include the external environment in approximate form, and we explore the effects that the external environment has on the cavity propagation rate.

TRANSPORT PROCESSES IN ONE-DIMENSIONAL CAVITIES WITH PASSIVE WALLS

The possibility of devising a simplified (yet physically realistic) description of the corrosion processes that occur within cavities can be demonstrated on the basis of a system that is very important from the practical point of view: the corrosion of iron in dilute chloride solutions. This system was widely investigated,[11] and we adopt all assumptions and equations that were described therein.

It is assumed that a single electrochemical reaction

$$Fe \rightarrow Fe^{2+} + 2e \tag{2}$$

takes place within the pit, and that the cavity contains six different ionic species, S_k

$$S_1 : Fe^{2+},\ S_2 : Fe(OH)^+,\ S_3 : Na^+,\ S_4 : Cl^-,\ S_5 : H^+,\ S_6 : OH^-$$

Additionally, three homogeneous reactions are assumed to occur

$$Fe^{2+} + H_2O = Fe(OH)^+ + H^+ \tag{3}$$

$$Fe(OH)^+ + H_2O = Fe(OH)_2(s) + H^+ \tag{4}$$

$$H_2O = H^+ + OH^- \tag{5}$$

with $Fe(OH)_2(s)$ representing the precipitated hydrolysis product. In the case of a deep

cylindrical pit (Fig. 1(a) and (b)) under steady-state conditions, the mass conservation equations are:

$$\frac{dN_k}{dx} = R_{Vk} + \frac{2N_{sk}}{a}, k = 1, ..., 6 \tag{6}$$

where N_k is the ionic flux density, x is the distance down the crevice, R_{Vk} is the rate of creation of species k per unit volume, and N_{sk} is the flux of species k at the metal–solution interface on the side walls. In the case of a parallel-sided crevice, we must substitute the width, w, instead of the radius of the pit, a, into equation (6). The homogeneous reactions are taken to be in equilibrium, and the equilibrium constants K_1, K_2 and K_w defined as

$$K_1 = c_2c_5/c_1, K_2 = c_5/c_2, K_w = c_5c_6. \tag{7}$$

If the walls of the pit or the crevice are ideally passive, all N_{sk} are equal to zero, but in the case of active walls, $N_{s1} = i_s/(2F)$, where i_s is the current density at the electrode and F is Faraday's constant. At this point, and in subsequent discussion, the subscript s refers to the electrode surface and m to the mouth of the pit or the crevice.

According to dilute solution theory, the molar flux of species k is given by the Nernst–Plank equation

$$N_k = -D_k\left(\frac{dc_k}{dx} + \frac{z_kF}{RT}c_k\frac{d\varphi}{dx}\right) \tag{8}$$

where c_k is the concentration of species k, D_k is the diffusion coefficient, z_k is the charge, T is the temperature, R is the gas constant, and φ is the electrostatic potential in the cavity. The solution is taken to be electrically neutral, so that

$$k = 1k = 6z_kc_k = 0 \tag{9}$$

The concentration and potential boundary conditions are written as

$$c_5 = 10^{-pH_b-3}, \quad c_6 = \frac{K_w}{c_5}, c_2 = \frac{c_5}{K_2}, \quad c_1 = \frac{c_2c_5}{K_1}, c_3 = c_b, c_4 = 2c_1 + c_2 + c_3 + c_5 - c_6,$$

$$\varphi = 0, \quad \text{at } x = 0 \tag{10}$$

where pH_b is the bulk value of the pH and c_b is bulk concentration of NaCl. At the crevice base, we have the following conditions for the fluxes:

$$N_i = -i_s/(2F), N_2 = N_3 = N_4 = N_5 = N_6 = 0; \text{ at } x = L \tag{11}$$

The electrodissolution reaction occurring in the cavity, due to oxidation of the metal, is described in terms of the Tafel equation as

$$i_s = i_0\exp\frac{\alpha F(V - U_0 - \varphi_s)}{RT} = i\exp-\frac{\alpha F\varphi_s}{RT}. \tag{12}$$

Here i_0 is the exchange current density, α is the anodic transfer coefficient, V is the electrode potential, U_0 is the open-circuit potential, φ_s is the electrostatic potential in the solution near the electrode surface, all referred to a reference electrode at infinity, and $i = i_0\exp aF(V - U_0)/RT$ is the current density calculated in the absence of a potential drop in the cell (the maximum possible current density on the electrode surface at the given potential of the metal).

After elimination of the terms R_{Vk}, the above system of equations was solved numerically in Ref.[11] using the finite element method for the solution, with $pH_b = 8$ and $c_b = 0.1$ M, for both active and passive walls. The calculated potential distributions were compared with experimental data,[23] and reasonable agreement was obtained.

The distributions of the species concentrations were not given in Ref.[11], so we had to devise our own code for solving this system of equations. We used a shooting method in combination with a the fourth-order Runge–Kutta algorithm. The integration steps were chosen to be very small (10^{-6} of the pit length) for the region near the mouth, where the solution properties change very sharply (for extremely dilute solution), but it was increased with increasing distance from the mouth. The value of the step size was chosen in such a manner that further reduction did not change the results. The parameters that were used in the numerical calculations are given in Table 1. All thermodynamic and kinetic data are taken from Ref.[11], where a SCE is used as the reference electrode.

Initially, the case of corrosion in a cavity with passive walls was investigated. It can be shown that the solutions to the coupled equations are functions of two independent variables (distance down the pit x, and the current density, i), but that they may be expressed as functions of a single independent variable, which is the product of current density and distance. The parameter xi was used,[8,9] for describing corrosion processes in one-dimensional cavities. As defined by Pilay and Newman[24] the product $q = xi$ represents the quasi-potential of the system. It can be shown[24] that under steady-state quiescent conditions, with equilibrium homogeneous chemical reactions, and for a single electrochemical reaction, the electrostatic potential and all concentration distributions can

Table 1. Parameters used in the calculations

Thermodynamic data
$K_1 = 10^{-9.8}$ mol/l
$K_2 = 10^{-4.9}$ mol/l
$K_{w'} = 10^{-13.98}$ (mol/l)^2
Diffusion coefficients
Fe^{2+}, $D_1 = 0.72 \times 10^{-5}$ cm^2/s
$Fe(OH)^+$, $D_2 = 1.0 \times 10^{-5}$ cm^2/s
Na^+, $D_3 = 1.334 \times 10^{-5}$ cm^2/s
Cl^-, $D_4 = 2.032 \times 10^{-5}$ cm^2/s
H^+, $D_5 = 9.302 \times 10^{-5}$ cm^2/s
OH^-, $D_6 = 5.3 \times 10^{-5}$ cm^2/s
Kinetic data
$i_{10} = i_0 \exp\{-U/RT\} = 1.96 \times 10^7$ A/cm^2
$\alpha = 1$
$T = 25$°C
$V = -0.58$ V (SCE)
Bulk solution data
$c_b = 0.1$ mol/l
$pH_b = 8$
Geometrical parameters
$a = 0.225$ cm
$L = 2.25$ cm

be represented as a single-valued harmonic function of the quasi-potential q. This harmonic function vanishes at infinity and satisfies the following boundary conditions

$$\frac{\partial q}{\partial n} = 0, \tag{13}$$

at an insulating surface, and

$$-\frac{\partial q}{\partial n} = i \tag{14}$$

at the electrode surface, where n is the unit normal vector at the electrode surface pointed towards the solution. Accordingly, all results that are represented as a function of $q = xi$ have general sense; they do not depend upon the geometry of the system and could be used, for example, for describing multi-dimension cases. From a mathematical point of view, the determination of the dependencies of the concentrations, c_k, and the electrostatic potential, φ, on the quasi-potential, q, is equivalent to the solution of the mass-transfer equations in a one-dimensional cavity.

Figure 2 shows the concentration profiles in a pit with passive walls. There are three species that dominate in the pit, Fe^{2+}, Cl^-, and Na^+, and only these species determine the electrostatic field in the cavity. Hence, if we only want to calculate the potential distribution in this system, we can approximate the complete system involving six species (Fe^{2+}, $Fe(OH)^+$, Na^+, Cl^-, H^+ and OH^-) by a reduced system involving only three species (Fe^{2+}, Na^+ and Cl^-).

As it follows from equation (6) and equation (9), the reduced ionic system is described by the following system of equations

$$N_1 = -\frac{i}{2F}, \quad N_3 = N_4 = 0, \quad 2c_1 + c_3 = c_4 \tag{15}$$

with the boundary conditions

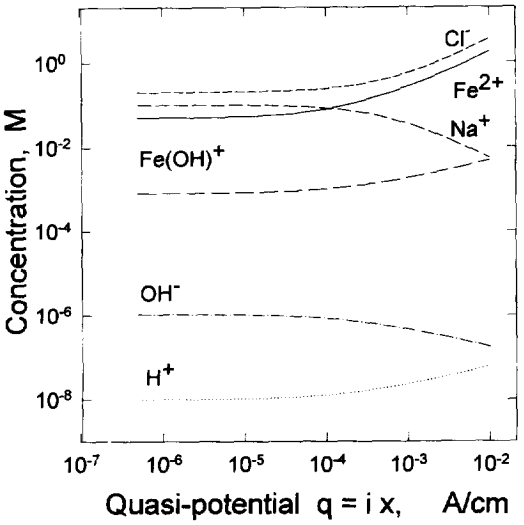

Fig. 2. The concentrations of species as a function of the quasi-potential in 0.1 M NaCl. The precipitation of $Fe(OH)_2$ is included.

$$c_4 = c_b^-, \quad c_3 = c_b^+, \quad c_1 = (c_b^- - c_b^+)/2, \varphi = 0, \text{ at } x = 0$$

where c_b^- and c_b^+ are the total bulk concentrations of anions and the non-active cations, respectively. We introduced these values for generality, in order to describe solutions in which the bulk concentration of $Fe(OH)^+$ is comparable to the concentration of Na^+. The analytical solution of this system can be easily found and has the form:

$$\varphi = \frac{RT}{F} \ln \frac{3 + \gamma + 2\varsigma q + \sqrt{(3 + \gamma + 2\varsigma q)^2 - 12\gamma}}{6} \tag{16}$$

$$c_4 = c_b^- \exp\left(\frac{F\varphi}{RT}\right), \quad c_3 = c_b^+ \exp\left(-\frac{F\varphi}{RT}\right), \quad c_1 = \frac{c_4 - c_3}{2} \tag{17}$$

where $\varsigma = 1/(2FD_1c_b^-)$ and $\gamma = c_b^+/c_b^-$. For the case where the cations of the dissolving metal (Fe^{2+}) are absent in the bulk (i.e. at $\gamma = 1$), the solution to the equation system (15) was obtained by Ateya and Pickering.[7] Equation (16) and equation (17) can be used to determine the concentrations of the other species, if they are of interest. In our case, they can be directly estimated from the equilibrium conditions equation (7) as

$$c_2 = \sqrt{K_1 c_1 / K_2}, \quad c_5 = K_2 c_2, \quad c_6 = K_w / c_5 \tag{18}$$

The numerically-obtained concentrations (Fig. 2) and potential (Fig. 3) differ from the analytical solutions that are given by equations (16)–(18) by less than 0.1%. It is interesting to note that the potential distribution differs little from that obtained for the case when only Fe^{2+} and Cl^- are present in the solution (i.e. in a binary system). For the binary electrolyte, putting $\gamma = 0$ in the equation (16) yields a much simpler expression:

$$\varphi = \frac{RT}{F} \ln\left\{1 + \frac{2}{3}\varsigma q\right\} \tag{19}$$

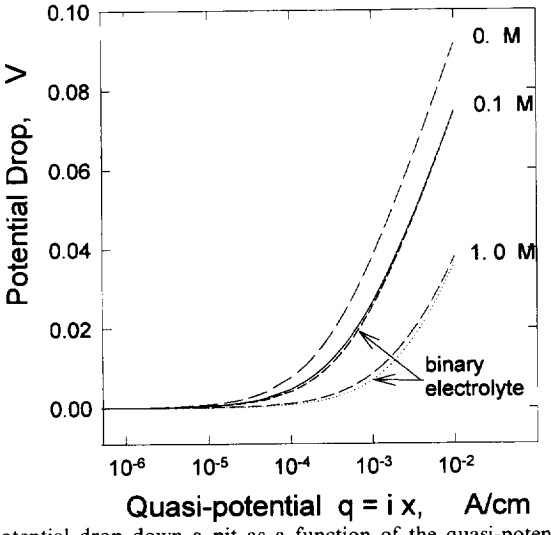

Fig. 3. The potential drop down a pit as a function of the quasi-potential for different bulk concentrations of NaCl. The precipitation of $Fe(OH)_2$ is included.

Equation (16) and equation (19) coincide for small and large values of ς and the maximum difference between these equations is found for at $\varsigma q \cong 1.25$ and does not exceed 2.25 mV at room temperature. This fact can be explained with the help of Figs 2 and 3. A significant potential drop is observed only for $q = ix > 1 \times 10^{-4}$ A/cm, and it is this region where all cations other than Fe^{2+} are expelled by the electric field and where Cl^- is concentrated for charge neutrality. Correspondingly, this binary system (Fe^{2+}, Cl^-) determines the potential drop in the cell.

equation (16) can also be used for describing the potential distribution if the precipitation of ferrous hydroxide is not taken into account (see equation (4)). This case can be very important for describing the corrosion processes in extremely dilute solutions, when Fe^{2+} and $Fe(OH)^+$ are not present in the bulk of the electrolyte, as is designated in the boundary conditions equation (10) employed in Ref.[11] Instead of equation (10), the following simple boundary conditions can be used:

$$c_5 = 10^{-pH_b-3}, c_6 = K_w/c_5, \quad c_1 = 0, c_2 = 0, c_3 = c_b, \quad c_4 = c_3 + c_5 - c_6, \quad \varphi = 0 \text{ at } x = 0$$

Our calculation (see Fig. 4) shows that the discrepancy between the analytical and numerical solutions does not exceed 1%, if the bulk concentration of NaCl is greater than 10^{-5} M at pH = 8 and is greater than 10^{-6} M for a neutral solution at (pH = 7). As one would expect, equation (16) (or equation (19)) describes with greater accuracy the potential distribution in the cavity if the bulk concentration of the principal anion (Cl^-) is much larger than the bulk concentrations of the other anions (in this case OH^-).

However, it can be shown that equation (16) (or equation (19)) can be used for the quantitative description of the potential drop in the cavity when the bulk concentration of the principal anion is comparable to (or even much less than) the concentrations of the other anions. As an example, consider the pitting of Zn(Me) in buffered diluted NaCl solution. This system was intensively studied in Ref.[9] The concentration and potential distribution

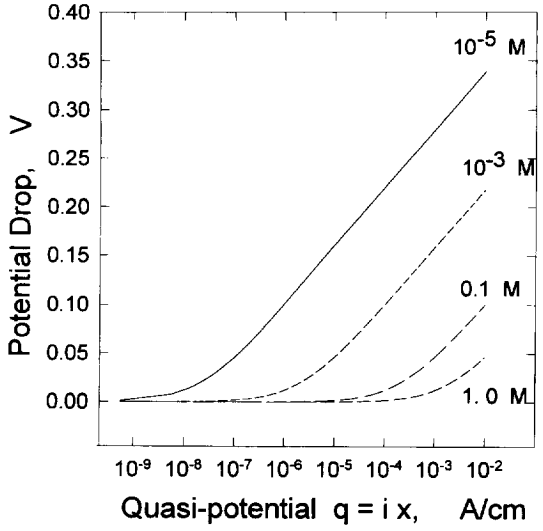

Fig. 4. The potential drop down a crevice as a function of the quasi-potential for different bulk concentrations of NaCl. The precipitation of $Fe(OH)_2$ is not included.

were calculated numerically for the solutions used in Ref.[25] Table 2 from Ref.[9] shows the compositions of the five solutions considered.

This system is much more complicated than the system described above. Four additional species in the solution

$$S_7 : \mathrm{Me(OH)_2(aq)},\ S_8 : \mathrm{Me(OH)_s(s)},\ S_9 : \mathrm{H_3BO_3},\ S_{10} : \mathrm{H_2BO_3^-}$$

and three additional chemical reactions

$$\mathrm{H_3BO_3} = \mathrm{H_2BO_3^-} + \mathrm{H^+} \tag{20}$$

$$\mathrm{NaCl} = \mathrm{Na^+} + \mathrm{Cl^-} \tag{21}$$

$$\mathrm{Me(OH)_2(aq)} = \mathrm{Me(OH)_2(s)} \tag{22}$$

were considered. In addition the chemical reaction

$$\mathrm{Me(OH)^+} + \mathrm{H_2O} = \mathrm{Me(OH)_2(aq)} + \mathrm{H^+} \tag{23}$$

takes place instead of equation (4).

The calculations show that, for sufficiently large value of quasi-potential $q = ix$ two species Zn^{2+} and Cl^- dominate in the solution (see Ref.[9]). In this case, without doing any special calculations for the potential, we can state that the potential distribution in the pit is described with great accuracy by equation (16) for the case of Solution I (Table 2). Figure 5 shows the potential distribution that was obtained numerically in Ref.[9] and the potential distribution from equation (16). We see that if the bulk concentrations of the principal anions is less than, or is comparable with the bulk concentration of $H_2BO_3^-$, equation (16) (or equation (19)) describes the numerical results quite accurately. Moreover, for many practical cases, we can use equation (19) for calculating of the potential distribution, even when the bulk concentration of the principal anion is less by an order of magnitude than the bulk concentrations of the other anionic species. The discrepancy, in this case, is less than 20 mV, and this discrepancy is found only for a definite value of the pit length. For sufficiently deep pits (sufficiently large value of $q = ix$), all potential distributions coincide, and the corrosion rates must be the same and are independent of the concentrations of the buffer species.

For practical calculations, for the case when the bulk concentration of the principal anion is less by an order of magnitude than the bulk concentrations of the other anionic species, it may be convenient to use the following approximation instead of equation (19) or equation (16) (see Fig. 5):

Table 2. Compositions of the bulk solutions

Solution number	NaCl (mol/l)	H_3BO_3 + NaH_2BO_3 (mol/l)	pH
I	2×10^{-2}	2×10^{-3}	9.2
II	2×10^{-2}	1×10^{-2}	9.2
III	2×10^{-2}	5×10^{-2}	9.2
IV	2×10^{-2}	1×10^{-1}	9.2
V	2×10^{-2}	2×10^{-1}	9.2

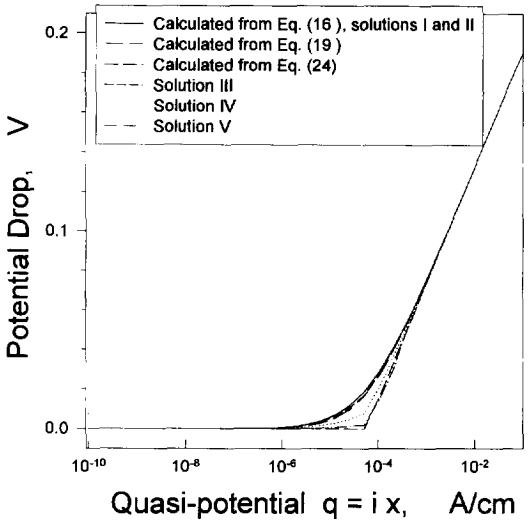

Fig. 5. The potential drop down a crevice as a function of the quasi-potential for the pitting of Zn in buffered NaCl solutions (see Table 2).

$$\varphi = 0 \text{ for } \varsigma q \leq 1.5 \text{ and } \varphi = \frac{RT}{F} \ln \frac{2}{3} \varsigma q \text{ for } \varsigma q > 1.5 \tag{24}$$

The maximum difference in the values of φ obtained from equations (19) and (24) is obtained when $\varsigma q = 1.5$ and equals $RT\ln\{2.18\}/F$ (0.020 V at room temperature). For deep pits, this difference vanishes. The physical sense of this approximation is that we neglect the potential drop that is present during the initial stage of the pit growth (i.e. when the pit is very small) and then use an asymptotic expression (equation (24)) to describe the potential drop within the crevice for dissolution of the metal in a cavity within an electrolyte of its own salt.

Figure 5 clearly shows that if we only wish to obtain information about the potential distribution near the electrode surface it can often be done with great accuracy for a large cavity (large q) by analyzing some simplified system (binary system for this case). Of course, a relatively larger error may be introduced into the determination of the potential distribution within the interior of the pit, but this error does not influence the value of the current density at the pit base. This method can give a very large relative error for very small cavities (very small q), but in small cavities the absolute value of the potential drop is normally so small that it has an insignificant influence on the current density. Accordingly, in this instance, the exact determination of the potential distribution may be not very important.

CALCULATION OF THE PIT GROWTH RATE

One of the steps in solving of mass transfer problems using the quasi-potential method is to estimate the current density on the electrode (pit) surface, i_s, as a function of the quasi-potential, q (see boundary condition equation (14)). In the general case, this task requires the solution of the mass-transfer equations in a one-dimensional cavity and, as noted above,

this can be rather complicated. However, as was also mentioned above, it is sufficient to know $i_s(q)$ only for large values of q and this information may be obtained by analyzing of a simplified system.

The expression for the current density at the electrode (pit) surface, i_s, as a function of the quasi potential, q, is obtained by substituting equation (16) into equation (12) to yield:

$$i_s = i\left\{\frac{3+\gamma+2\varsigma q+\sqrt{(3+\gamma+2\varsigma q)^2-12\gamma}}{6}\right\}^{-\alpha} \tag{25}$$

Using equation (19) we obtain another, more simple expression:

$$i_s = i\left\{1+\frac{2}{3}\varsigma q\right\}^{-\alpha} \tag{26}$$

The difference between the values of the current density, i_s, that is obtained from equation (25) (at $\gamma = 1$) and that given by equation (26) does not exceed 9%.

In the case of a one-dimensional pit with passive walls, the quasi-potential at the tip of the pit equals $i_s L$ and equation (25) (or equation (26)) yields the function $i_s = i_s(L)$ in implicit form. As follows from equation (25), the ratio of the current density, i_s, to the current density calculated in the absence of a potential drop in the cell, i, depends only on the parameters $A = \zeta iL$, α, and γ. This equation has no analytical solution for an arbitrary value of α, but it is easy to solve for small and large values of the parameter A. For $A < 1$, the expression in brackets in equation (25) approximately equals 1, but for $A \gg 1$ it approximately equals $2\varsigma q/3$. Accordingly, we have:

$$i_s = i \text{ for } \varsigma iL < 1 \tag{27}$$

and

$$i_s = \frac{i}{(2\zeta iL/3)^{\alpha/(1+\alpha)}} \text{ for } \varsigma iL \gg 1 \tag{28}$$

The form of these limits suggests a simple interpolation formula, as follows

$$i_s = \frac{i}{(1+2\zeta iL/3)^{\alpha/(1+\alpha)}} \tag{29}$$

which can be used for any arbitrary value of the parameter $A = \zeta iL$. Figure 6 illustrates the accuracy of the interpolation equation.

Using Faraday's law, we can write the growth rate of the cavity as

$$\frac{dL}{dt} = \frac{M_m i}{\rho_m 2F} \tag{30}$$

where M_m and ρ_m are the molecular weight and the density of the metal, respectively. Substitution of equation (29) into equation (30) and integration for the boundary condition $L = 0$ at $t = 0$ yields:

$$L = L_0\left[\left(1+\frac{t}{t_0}\right)^m - 1\right] \tag{31}$$

where the power, m, has the form

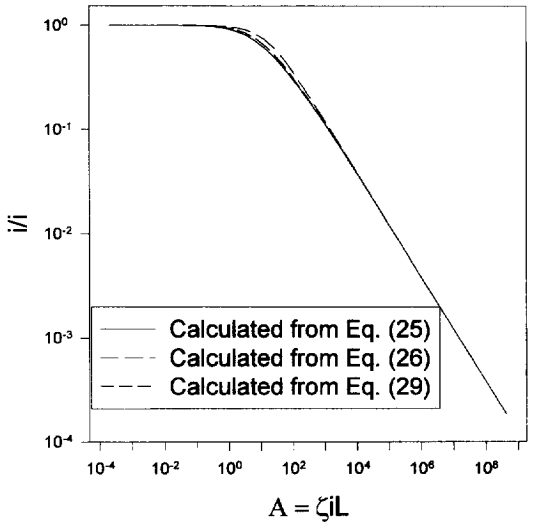

Fig. 6. The relative current densities as the function of the pit length for $\alpha = 1$, calculated numerically from equation (25) with $\gamma = 1$, from equation (26), and from equation (29).

$$m = \frac{\alpha + 1}{2\alpha + 1} \tag{32}$$

and

$$L_0 = \frac{1}{(2\varsigma i/3)}, \; v_0 = \frac{M_m i}{\rho_m 2F}, \; t_0 = \frac{mL_0}{v_0} \tag{33}$$

For small times ($t < t_0$) when the potential drop has an insignificant influence on the current density, as follows from equation (31), L can be represented as the linear function of t

$$L = v_0 t \tag{34}$$

and for large times ($t \gg t_0$), L takes the form of equation (1)

$$L = L_0 \left(\frac{t}{t_0}\right)^m = kt^m$$

where m is given by equation (32) and k is given by the following expression:

$$k = L_0 \left(\frac{1}{t_0}\right)^m = \left(\frac{2\alpha + 1}{\alpha + 1} \frac{M_m}{\rho_m 2F}\right)^{\frac{\alpha+1}{2\alpha+1}} (3FD_1 c_b^-)^{\frac{\alpha}{2\alpha+1}} (i)^{\frac{1}{2\alpha+1}} \tag{35}$$

If α is equal 1 (as is suggested in Ref.[11]), m is equal to 2/3. This means that the very frequently observed case of $m = 2/3$ can be explained by presence of a non-linear potential distribution inside the pit (see equation (19)).

The velocity of pit propagation is obtained by differentiating equation (31) to yield

$$v = \frac{\mathrm{d}L}{\mathrm{d}t} = v_0 \left(1 + \frac{t}{t_0}\right)^n \tag{36}$$

where

$$n = m - 1 = -\frac{\alpha}{2\alpha + 1}. \tag{37}$$

Thus,

$$v = v_0, \text{ at } t/t_0 < 1, \text{ and } v = v_0(t/t_0)^n \text{ for } t/t_0 \gg 1. \tag{38}$$

Furthermore, as it follows from the equation (35), for sufficiently large time, the pit growth rate is proportional to $(c_b^-)^{\frac{\alpha}{2\alpha+1}}$, and in particular, at $\alpha = 1$, we have $v \propto \sqrt[3]{c_b^-}$.

All relations that are listed above can be easily modified for the case where anions are involved directly in the anodic reactant. The effect of solution composition on metal dissolution processes and, in particular, on the kinetics of localized corrosion, has been clearly established. Some aggressive anions, such as Cl^-, Br^-, and I^-, exhibit specific activities towards metal dissolution.[21,36] The dissolution of metal, Me, to produce stable complexes

$$\text{Me} + qA^- = [\text{Me}A_q]^{n-q} + ne^- \tag{39}$$

provides the simplest example of electrochemical systems in which there is a direct influence of anions A^- on the rate of the electrode reaction.

In some cases, anions can influence the kinetics of some intermediate stage of the anodic dissolution process, and thus affect the rate of the entire process if the stage affected occurs before the rate determining step. For example, as is noted in Ref.[27], the dissolution of metals in pits, which takes place according to the overall reaction

$$\text{Me} \rightarrow \text{Me}^{n+} + ne^- \tag{40}$$

consists of three successive, non-equilibrium reactions, with the first being described by equation (39). Subsequent steps are considered to be

$$[\text{Me}A_q]^{n-q} + s\text{H}_2\text{O} = [\text{Me}A_q(\text{H}_2\text{O})_s]^{n-q} \tag{41}$$

and

$$[\text{Me}A_q(\text{H}_2\text{O})_s]^{n-q} = \text{Me}^{n+} + qA^- + s\text{H}_2\text{O} \tag{42}$$

In either case, the rate of dissolution can be approximated by a Tafel kinetic expression

$$i = k_a C_{As}^{\lambda} \exp\left\{\frac{\alpha F(V - U - \varphi_s)}{RT}\right\} \tag{43}$$

where C_{As} is the surface concentration of the aggressive anion, k_a is the rate constant for the reaction proceeding in the anodic direction, and λ is the effective kinetic order of the metal dissolution reaction with respect to the anion concentration. The value of λ is usually restricted to $0 \leq \lambda \leq 1$.[21] In steady-state, non-convective electrolytic systems, the anion species can be regarded as motionless if this species does not participate in any entire electrochemical or homogeneous chemical reaction. Accordingly, the concentration of an anion can be described by the Boltzmann expression

$$C_{As} = C_{Ab} \exp -F\varphi_s/RT \tag{44}$$

where C_{Ab} is the concentration of aggressive anions in the bulk of the solution. It follows

from equations (43) and (44) that the dissolution rate at the pit can be represented by an expression in the form of equation (12)

$$i = i\exp\left\{-\frac{\alpha_{ef}F\varphi_s}{RT}\right\}, \tag{45}$$

where effective anodic transfer coefficient, α_{ef}, is introduced as follows,

$$\alpha_{ef} = \alpha - \lambda \tag{46}$$

It is evident that all equations are still valid if we formally change α to $\alpha_{ef} = \alpha - \lambda$ in region $\alpha_{ef} > -0.5$ to insure a positive value of power m. The case where $\alpha_{ef} \leq -0.5$ can lead to the instability of the process and requires attention that is beyond the scope of this paper.

In summary, three essentially different cases of pit propagation are predicted:

1. $\alpha > \lambda$, i.e. $\alpha_{ef} > 0$. This is a common case. Since the value of electric potential, φ_s, at the bottom of the pit increases as the pit propagates, the dissolution rate at the bottom decreases as a function of pit depth, L (or time, t) according to equation (29) (or equation (36)).
2. $\alpha = \lambda$, i.e. $\alpha_{ef} = 0$. In this case, the accelerating action of anions on the electrode reaction completely compensates for the increasing potential drop in the solution during pit growth. The dissolution rate does not change with pit length or time and equals v_0.
3. $\alpha < \lambda$, i.e. $\alpha_{ef} < 0$. In this case, the accelerating action of anions on the electrode reaction outweighs the inhibiting effect that is related to the increase in the potential drop in the crevice environment, as the pit grows. Acceleration of the pit growth rate with time has been noted in the literature. Thus, as shown in Ref.[22], where data for a variety of materials under different experimental conditions are summarized, the exponent, n, ranges from -0.7 to 0.4. It follows from equation (37), that when the anodic transfer coefficient, α_{ef}, is in the region $-0.222 < \alpha_{ef} < 0$. the exponent, n, has values $0 < n < 0.4$, corresponding to the acceleration of pit growth rate with time (or depth).

THE INFLUENCE OF EXTERNAL ENVIRONMENT

It has been tacitly assumed, so far in our calculations, that in the case of a sufficiently deep pit, it is possible to neglect the potential drop in the external environment and to calculate the potential distribution, φ, by solving the balance equations inside the pit only. Using the concept of the quasi-potential, the validity of this assumption can be demonstrated in the case of pits with passive walls in an absolutely motionless electrolyte, where the presence of the diffusion layer (with higher values of concentrations than in the bulk of the solution) near the pit mouth reduces the resistance of the local external environment to charge transfer. In the case of the moving electrolyte, we assume that the velocity is high enough that significant concentration gradients do not exist in the bulk solution. Accordingly, the distribution in the potential in the external environment can be found by solving Laplace's equation for the electrostatic potential, φ, subject to nonlinear boundary conditions (in the general case) that correspond to the kinetics of reduction of a cathodic depolarizer (e.g. O_2).

It is convenient to represent the average potential at the pit mouth, φ_m, in the form of

$$\varphi_m = C\frac{i_m a}{\kappa} \tag{47}$$

as determined by dimensional analysis, where i_m is the current density at the pit mouth, κ is

the conductivity, and the dimensionless parameter C can be estimated, as shown below. It is evident that the external environment presents a maximum resistance to charge transfer if the outer surface of the metal is isolated and the current is forced flow to infinity. The solution to Laplace's equation for this case is well known,[28] and yields $C_{max}=8/3\pi$. The external environment presents minimum resistance to charge transfer when the electrode reactions on the external metal surface can occur close to the cavity mouth and are kinetically fast. In this case, the surface overpotential is negligible compared to the ohmic potential drop in the solution. The solution to Laplace's equation for this case is also known,[28] and yields $C_{min}=4/3\pi$. It is convenient to choose a mean value for C as

$$C = (C_{min} + C_{max})/2 = 2/\pi \tag{48}$$

in order to estimate the potential at the crevice mouth, φ_m, for the general case. The uncertainty introduced into C will not result in an uncertainty in φ_m exceeding 50%, and this error is independent of the law of polarization governing the cathodic reactions on the external surface. We must emphasize that this uncertainty does not translate into a comparable uncertainty in the pit propagation rate (the uncertainty in the latter is much smaller). If the current density at the mouth of the pit, in case of a the moving electrolyte, is obtained without taking into account the potential drop in the external environment (outside the pit), the validity of this assumption can be checked by using equation (47). In very dilute moving electrolytes, the potential drop outside of the cavity, φ_m, in a moving electrolyte, can be comparable with the potential drop in the cavity, and, therefore, processes occurring on the external surfaces must be taken into account even for a deep pit.

For cracks and crevices (i.e. slots), the potential drop outside of the cavity can be much higher than for a cylindrical pit. For this case (i.e. crevices), we will continue to represent the potential drop in the solution in the form of equation (47) by changing the radius of the pit to the width of the crevice, w. Using the results,[29] it can be shown that $C_{min}=\pi/8$. The parameter, C_{max}, can be calculated if we assume that the crevice has a finite thickness, d. In this case, the expression for C_{max} has the form:[28]

$$C_{max} = \frac{1}{\pi}\left\{\sinh^{-1}\frac{d}{w} + \frac{d}{w}\sinh^{-1}\frac{w}{d} + \frac{1}{3}\left\{\frac{w}{d} + \frac{d^2}{w^2} - \left(\frac{d^{4/3}}{w^{4/3}} + \frac{w^{2/3}}{d^{2/3}}\right)^{3/2}\right\}\right\} \tag{49}$$

For example, if $w=10\,\mu m$, and $d=1\,cm$, we have $C_{max}=2.349$. It is evident that $C_{max}\to\infty$, when $d/w\to\infty$. Thus, the ohmic drop in a moving electrolyte can be much larger in the case of crevice corrosion than it is in the case of pitting corrosion. Under some conditions, the transport processes in the external environment can control completely the kinetics of cavity growth.

Figure 7 shows the calculated change in the depth of a hypothetical cylindrical pit, having passive walls and a radius 50 μm, with time. The calculations were performed numerically, taking into account the potential drop in the external environment. For each step in the solution of equation (30), the current density in the crevice was determined from the equation

$$\varphi_s(i) = \varphi_m(i) + \Delta\varphi_{in}(i) \tag{50}$$

Here the dependencies of the potential drop in the solution, $\varphi_s(i)$, the potential drop in the external environment, $\varphi_m(i)$, and the potential drop inside the pit, $\Delta\varphi_{in}(i)$, on the current

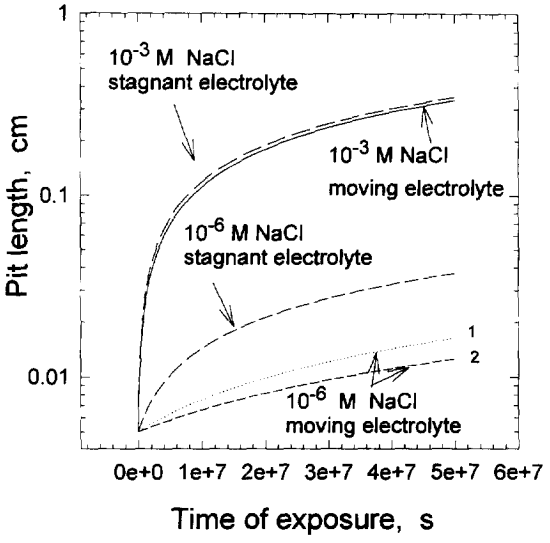

Fig. 7. Pit depth as a function of time. (a) rapid cathode reaction on the external surfaces, (b) with the outer surface of the metal being isolated. Precipitation reaction is not included.

density are determined from equation (12), equation (47) and equation (16) (or equation (19)), respectively.

The numerical results for stagnant electrolytes are very close to the analytical solution given by equation (31) (the discrepancy is not visible on the scale employed here). However, there is a significant difference between the kinetics of pit growth in stagnant and moving electrolytes at low electrolyte concentrations. We also see that the approximation in equation (48) applies to this case. By using equation (48), the results lie approximately midway between the Curves 1 and 2, and the resulting error is less than 15% and is independent of the law of polarization of the cathodic reactions on the external surfaces.

It is useful to quantify conditions under which we can neglect, or must take into account, transport processes in the external environment when estimating the crevice propagation rate. By analogy with current distributions on polarized electrodes,[30,31] we introduce the dimensionless parameter:

$$\mathrm{Wa} = \frac{\partial \Delta\varphi_{\mathrm{in}}}{\partial i_{\mathrm{m}}} \Big/ \frac{\partial \varphi_{\mathrm{m}}}{\partial i_{\mathrm{m}}} \tag{51}$$

(an analog of the Wagner parameter), which represents the ratio of the resistance of the internal environment to the resistance of the external environment. Here, i_{m} is the current density at the mouth of the pit. If $\mathrm{Wa} < 1$, then charge transfer in the external environment determines the current density in the system, and when $\mathrm{Wa} > > 1$, transport processes in the cavity determine the current. For the case of the stagnant electrolyte, it can be easily shown that $\mathrm{Wa} = L/(Ca)$ (for $L > > a$), and $\mathrm{Wa} > > 1$ if the condition $L > > a$ exists. This means, as was previously mentioned, that in the case of a deep pit with passive walls in the stagnant electrolyte we can neglect the resistance of the external environment.

Using equation (19), which can be rewritten in the form, $\Delta\varphi_{\mathrm{in}} = (RT/F)\ln(1 + 2i_{\mathrm{m}}L/3)$ and equation (47), we have

$$\mathrm{Wa} = \frac{RT}{F}\frac{1}{i_m}\frac{\kappa}{Ca} \tag{52}$$

Figure 8 shows the influence of the bulk concentration of NaCl on the current density at the tip of a pit with passive walls (the parameters used in this calculation correspond to iron). Using equations (25) and (52), we can calculate that Wa changes from 3.5 to 0.014 when the bulk concentration of NaCl changes from 0.1 M to 10^{-6} M. Accordingly, a significant influence of the external environment on the corrosion growth rate is observed for low bulk concentration of the electrolyte.

CORROSION PROCESSES IN DEEP PITS WITH ACTIVE WALLS AND IN HEMISPHERICAL PITS

The case of a deep pit or crevice with active walls (Fig. 1(b)) can be easily described using the concept of the quasi-potential. If we average the Laplace's equation over the pit cross-section, the equation for determining the quasi-potential, q, has the form

$$\frac{d^2q}{dx^2} = -\frac{2i_s(q)}{a} \tag{53}$$

which must be solved subject to the following boundary conditions

$$q = 0 \text{ for } x = 0, \tag{54}$$

and

$$\frac{dq}{dx} = i_s(q) \text{ for } x = L \tag{55}$$

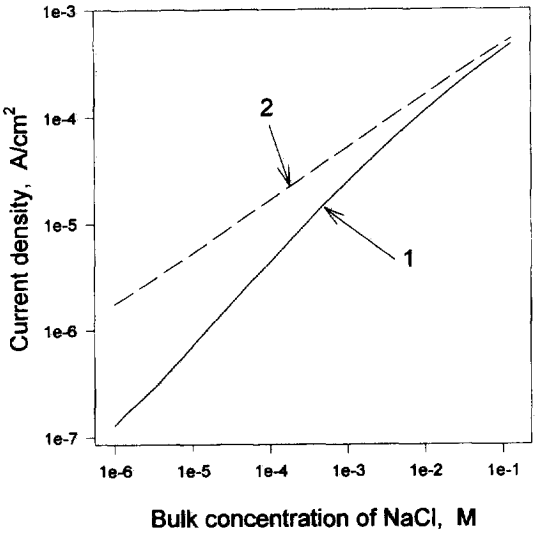

Fig. 8. The current density in the pitting of Fe with passive walls in a moving NaCl electrolyte (Curve 1). Curve 2 was calculated without taking into account the potential drop outside the pit. pH = 7, and other physical and geometrical parameters were taken from Table 1. Precipitation reaction is not included. Outer surface of the metal is isolated.

where $x = 0$ corresponds to the point on the pit axis at the pit mouth. The expression for the current density at the pit surface, i_s, as a function of the quasi-potential, q, is obtained from equation (25) (or equation (26)).

equation (53) represents an equation with separable variables and has the well-known solution:

$$\int_0^q \frac{\mathrm{d}q}{\sqrt{(2/a)\int i(q)\mathrm{d}q + C}} = x \tag{56}$$

where constant C can be found from the boundary condition given by equation (55). Unfortunately, $q(x)$ cannot be expressed through elementary functions for an arbitrary value of the transfer coefficient, α. However, the numerical solution of equation (53) is much simpler that the solution of the system of equations (6)–(9).

After finding the solution, $q(x)$, the potential distribution in the cavity and current density on the active pit wall, i_s, can be found by using equation (16) (or equation (19)) and equation (25) (or equation (26)). As an example, Fig. 9 shows the distribution in the current density on the active wall for the dissolution of Fe in a moving NaCl electrolyte. The geometrical and other parameters are taken from Table 1. We see that, in this case, the external environment exerts a more dramatic influence on the corrosion rate in the cavity than it does in the case of the pit with passive walls. Significant influence is observed even for a moderately dilute solution (0.1 M) and the difference increases to more than two orders of magnitude for extremely dilute solutions (10^{-6} M). The inescapable conclusion is that quantitative description of the propagation of a pit with active walls in a moving electrolyte requires in the general case consideration of the resistance of the external environment.

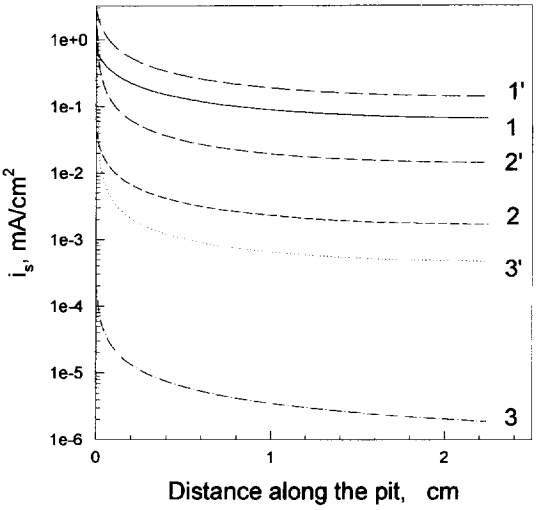

Fig. 9. The current density on the active wall in the pitting of Fe in a moving NaCl electrolyte with concentrations: 1–0.1 M, 2–10^{-3} M and 3–10^{-6} M. Curves 1′, 2′ and 3′ were calculated without taking into account the potential drop outside the pit for the corresponding bulk concentrations of NaCl. pH = 7, and other physical and geometrical parameters were taken from Table 1. The precipitation reaction is not included. The outer surface of the metal is isolated.

This important conclusion can be explained in terms of the Wagner number. Substituting $i_{av} = i_m a/(2L)$ into the right side of equation (51), instead of $i_s(q)$, and integrating the resulting equation with the simplified boundary condition, $(dq/dx) = 0$ for $x = L$ (i.e. we neglect the current that flows from the pit tip, which is small compared with the total current), we obtain the following expression for the potential drop in the cavity.

$$\Delta\varphi_{in} = \frac{RT}{F} \ln\{1 + 2\varsigma i_m L/3\} \tag{57}$$

Substituting equation (47) and equation (57) into equation (51) yields an expression for the Wagner number, which coincides with that given by equation (52). We see that the potential drop in the external environment increases in importance in the case of a pit (crevice) with active walls, because the current density at the pit mouth can be orders of magnitude larger than that at the pit tip.

Of course, the influence of the external environment on the rate of pit (crevice) growth must decrease with increasing pit length. However, due to the rather flat dependence of the current density on the active walls from the distance along the pit (with exemption for the narrow region near the pit mouth—see Fig. 9) the dependence of cavity growth rate on L is not very sharp. Thus, Fig. 10 shows the influence of the pit length, L, on the average current density in a pit with active walls exposed to a moving 10^{-3} M NaCl electrolyte for 0.1 cm $\leq L \leq 1$ cm. The value chosen for the pit radius, a, is 0.01 cm which provides the condition $a < L$. We see that, although the relative error incurred by neglecting the external environment does not decrease significantly with the increasing L, neglect of the external environment gives rise in the pit growth rate of a factor of about 10.

As the last example of the application of the method described above, we consider the essentially two-dimensional system of a hemispherical pit (Fig. 1(c)). For a sufficiently large pit, the quasi-potential satisfies the following boundary conditions

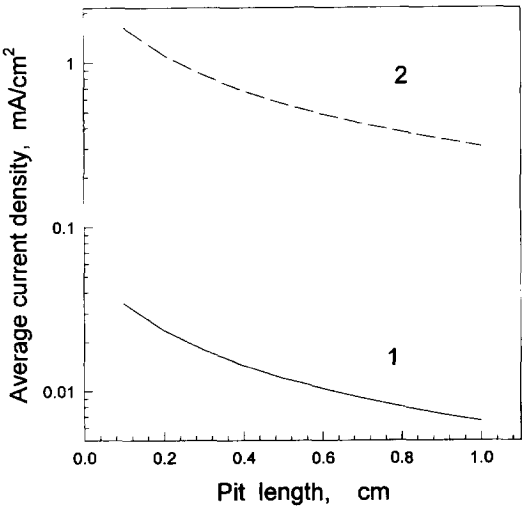

Fig. 10. The average current density in a pit with active walls in a moving 10^{-3} M NaCl electrolyte as a function of pit length (Curve 1). Curve 2 was calculated without taking into account the potential drop outside the pit. Radius of the pit is 0.01 cm, pH = 7, and other physical and geometrical parameters were taken from Table 1. Precipitation reaction is not included. The outer surface of the metal is isolated.

$$\frac{dq}{dn} = i\left(\frac{2}{3\varsigma q}\right)^{\alpha} \text{ at the electrode surface, and } \frac{dq}{dn} = 0 \text{ at an insulator.} \tag{58}$$

Introducing the dimensionless quasi-potential $Q = q/q_0$, where $q_0 = (ia)^{\frac{1}{\alpha+1}}\left(\frac{2}{3}\varsigma\right)^{-\frac{\alpha}{\alpha+1}}$, and normalizing all distances to the radius of the hemisphere, we can represent the current density at the pit surface in the following form

$$i = \frac{q_0}{a} Q^{-\alpha}, \tag{59}$$

where the dimensionless quasi-potential Q is a harmonic function that vanishes at infinity, and satisfies the boundary conditions $\frac{dQ}{dn} = Q^{-\alpha}$ at the surface of a hemispherical pit of unit radius and $\frac{dQ}{dn} = 0$ at an insulator. Correspondingly, the average current density, i_{av}, can be represented in the following form

$$i_{av} = \frac{q_0}{a} Q_{av}^{-\alpha} = i\left(\frac{2}{3}\varsigma ia\right)^{-\alpha/(\alpha+1)} Q_{av}^{-\alpha}, \tag{60}$$

where $Q_{av}^{-\alpha}$ is the average value of $Q^{-\alpha}$ on the surface of the pit, which depends only on parameter α. This value was calculated numerically by solving Laplace's equation with non-linear boundary conditions using the boundary element method (see Fig. 11). The results can be approximated by the following dependence

$$Q_{av}^{-\alpha} = 2.4/\sqrt[3]{1 + 2.4\alpha} \text{ for } -0.25 \leq \alpha \leq 1.5. \tag{61}$$

Figure 12 shows the application of equation (60) for describing of a single pit polarization curve for Ni dissolution in 0.5 M NaCl. In the given interval of polarization, the solution near the cavity surface becomes highly concentrated[16,17] and the theory of transport phenomena in concentrated solutions must be applied. Among other factors, the

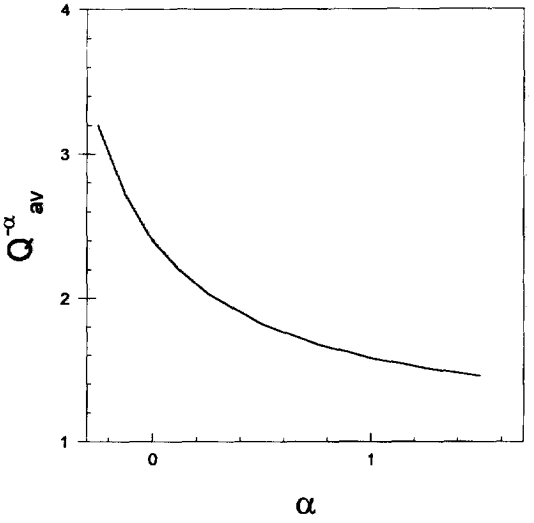

Fig. 11. The value $Q_{av}^{-\alpha}$ as a function of α.

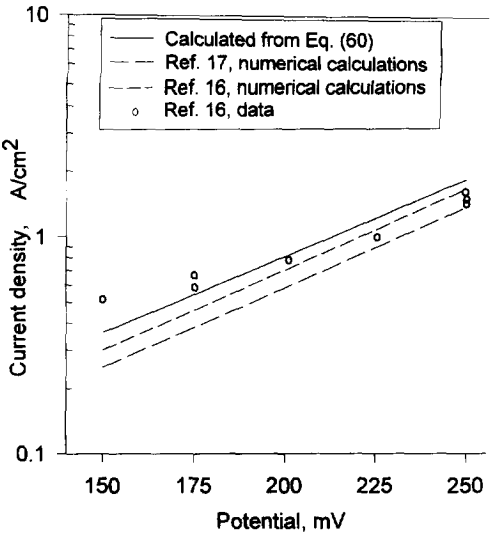

Fig. 12. The average pit current density vs applied potential (SCE) for dissolution of a hemispherical nickel pit of radius 30 μm in 0.5 M NaCl. Parameter values are taken from [15,17] (see Table 3).

chemical complexation reactions of Ni^{2+} with Cl^- are of great importance. However, as we can see from Fig. 12, the analytical expression equation (60) can be used for scoping calculations, even for the case of concentrated solutions. By analogy with a one-dimensional pit, it is easy to define an expression for the average pit radius, a_{av}, for sufficiently large t in the form of equation (1), with m given by equation (32), and

$$k = \left(\frac{2\alpha+1}{\alpha+1}\frac{M_m}{\rho_m 2F}\right)^{\frac{\alpha+1}{2\alpha+1}} (3FD_1 c_b^-)^{\frac{\alpha}{2\alpha+1}} (i)^{\frac{1}{2\alpha+1}} (Q_{av}^{-\alpha})^{\frac{\alpha+1}{2\alpha+1}}. \tag{62}$$

For the initial stages of pit growth $m = 1$, can be used. The cases of $m = 2/3$ and $m = 1$ are commonly observed in the growth of hemispherical pits.[2]

SUMMARY AND CONCLUSIONS

The analysis of corrosion in cavities as presented above, demonstrates that it is only necessary to take into account those species in the solution that determine the potential distribution near the electrode surface when calculating the cavity growth rate. This generalization significantly simplifies the mathematical description of localized corrosion processes, and even allows us to obtain, in some cases, analytical expressions for the cavity growth rate that can be used in engineering practice. The advantage of this method is that it permits one to predict the rates of cavity propagation without knowing various parameters that are often difficult to obtain, such as the equilibrium constants of some chemical reactions and the diffusion coefficients for species of relatively low concentration. Thus, it is possible to ignore chemical reactions, such as the hydrolysis of metal cations produced by the anodic reaction and the autoprotolysis of water, when describing the corrosion of iron in

neutral sodium chloride solutions, if the concentration of NaCl is greater than about 10^{-6} M. The analytical expressions, which were obtained in this paper, can be used for the quantitative description of pit propagation in dilute solutions; for example, for estimating damage functions, but they can also be used for scoping calculations in the case of highly concentrated solutions. It is shown that the very frequently observed case of the dimension of a pit being proportional $t^{2/3}$ can be explained by the presence of a non-linear potential distribution inside the pit. The influence of aggressive anions on the cavity propagation rate was also investigated. An important finding of this work is that transport processes in the external environment do, in the general case, influence the kinetics of cavity propagation. This influence is especially significant for the case of a deep cavity with active walls in a moving electrolyte. The method developed for analyzing these cases may be useful for describing not only corrosion processes, but also for defining processes in electrochemical technology, such as electrochemical etching and machining.

In this article, we restricted ourselves to cases, that were taken from literature, were a single electrochemical reaction occurs within the pit. However, it is apparent that the method is applicable to cases where multiple electrochemical reactions occur at the dissolving surface.

Acknowledgement—The authors gratefully acknowledge the support of this work by the Electric Power Research Institute under Contract #RPS520-13.

REFERENCES

1. S. M. Sharland, *Corros. Sci.* **27**, 289 (1987).
2. A. Turnbull, *Br. Corros. J.* **28**, 297 (1993).
3. H. S. Isaacs, *J. Electrochem. Soc.* **120**, 1456 (1973).
4. J. V. Tester and H. S. Isaacs, *J. Electrochem. Soc.* **122**, 1438 (1975).
5. R. Alkire, D. Ernsberger and D. Damon, *J. Electrochem. Soc.* **123**, 456 (1976).
6. H. W. Pickering and R. P. Frankenthal, *J. Electrochem. Soc.* **119**, 1297 (1972).
7. D. G. Ateya and H. W. Pickering, *J. Appl. Electrochem.* **11**, 453 (1981).
8. J. R. Galvele, *J. Electrochem. Soc.* **123**, 464 (1976).
9. S. M. Gravano and J. R. Galvele, *Corros. Sci.* **24**, 517 (1984).
10. S. M. Sharland and P. W. Tasker, *Corros. Sci.* **28**, 603 (1988).
11. S. M. Sharland, C. P. Jackson and A. J. Diver, *Corros. Sci.* **29**, 1149 (1989).
12. J. C. Walton, *Corros. Sci.* **30**, 915 (1990).
13. J. C. Walton, G. Grangolino and S. K. Kalandros, *Corros. Sci.* **38**, 915 (1990).
14. J. Newman, D. N. Hanson and K. Vetter, *Electrochim. Acta* **22**, 829 (1977).
15. M. V. Verbrugge, D. R. Bakker and J. Newman, *Electrochim. Acta* **38**, 1649 (1993).
16. J. N. Harb and R. C. Alkire, *J. Electrochem. Soc.* **138**, 2594 (1991).
17. M. V. Verbrugge, D. R. Bakker and J. Newman, *J. Electrochem. Soc.* **140**, 2530 (1993).
18. D. D. Macdonald and M. Urquidi-Macdonald, *Corros. Sci.* **32**, 51 (1991).
19. D. D. Macdonald, C. Liu and M. Urquidi-Macdonald, *Corrosion* **50**, 761 (1994).
20. Z. Szklarska-Smialowska, Pitting Corrosion of Metals, National Association of Corrosion Engineers, Houston (1986).
21. L. I. Freiman, Progress in Science and Technology. Corrosion and Corrosion Protection [in Russian], **11**, VINITI, 3 (1985).
22. D. D. Macdonald, C. Lui, M. Urquidi-Macdonald, G. H. Sickford, B. Hindin, A. K. Agrawal and K. Krist, *Corrosion* **50**, 761 (1994).
23. J. A. Beavers and N. G. Thompson, *Corrosion* **43**, 185 (1987).
24. B. Pilay and J. Newman, *J. Electrochem. Soc.* **140**, 414 (1993).
25. J. Augustynski, F. Dalard and J. C. Sonm, *Corros. Sci.* **12**, 713 (1972).
26. J. Tousek, *Corros. Sci.* **15**, 147 (1975).

27. Yu. A. Popov, Y. V. Alekseev and Ya. M Kolotyrkin, *Electrokhimia* **14**, 1147 (1978).
28. H. S. Carslaw and J. C. Jaeger, *Conduction of Heat in Solids*, 2nd edn. Oxford Press, London (1959).
29. C. J. Tranter, *J. Appl. Phys.* **24**, 369 (1953).
30. T. P. Hoar and J. N. Agar, Discuss. Faraday Soc. **1**, 162 (1947).
31. C. Wagner, *J. Electrochem. Soc.* **98**, 116 (1951).